Oregon State University OSU

Ph.D. Final Oral Examination

Studying fusion reactions

for effect of P_{CN} on heavy nucleus formation

and

for nuclear structure effects

October 11, 2007

Radhika Naik
Department of Chemistry
Oregon State University

Oregon State University OSU

Overview

- Introduction

- Determination of P_{CN} in $^{50}Ti + ^{208}Pb$ fusion reaction
  - Background and motivation
  - Experimental details
  - Data analysis and results
  - Future work

- Sub-barrier fusion of ^{9}Li with ^{70}Zn
  - Background and motivation
  - Experimental details
  - Data analysis and results
  - Future work

Introduction

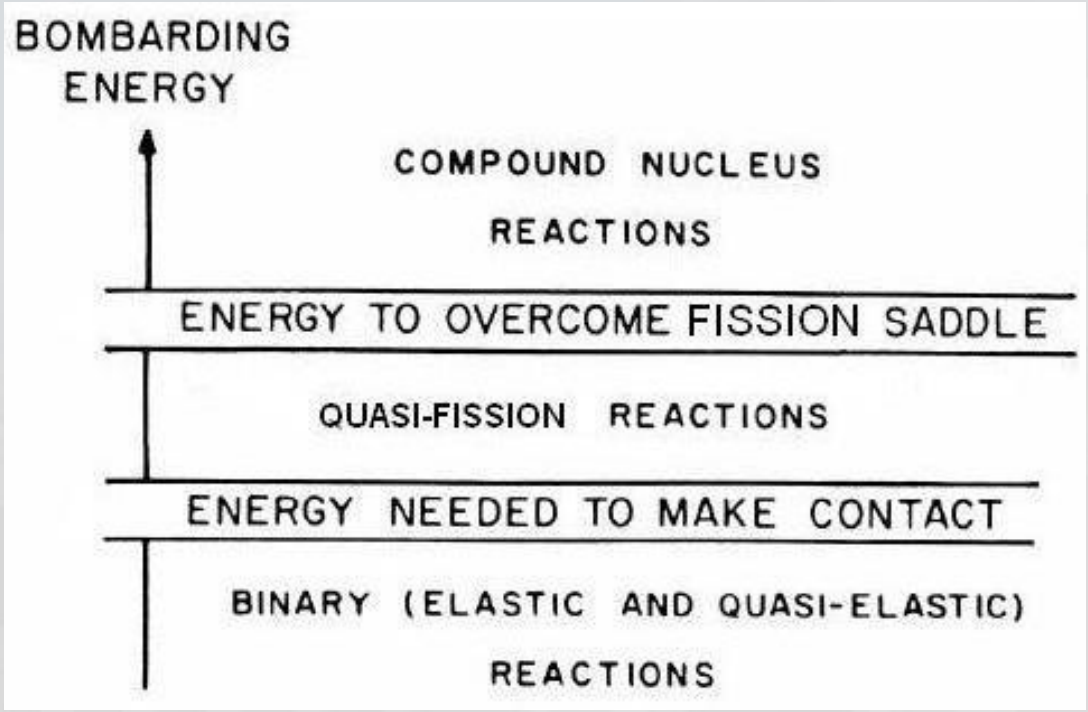

Compound nucleus:

A relatively long-lived reaction intermediate that is a result of complicated set of two-body interaction in which energy of projectile is distributed among all the nucleons of the composite system *(Loveland 2005)*.

Introduction (contd.)

- Variation of nuclear potential as a function of angular momentum (*l*) and radial separation (R).
- At lower *l*, there are "pockets" in the potential curve which signify the combination of potential and radial separation at a given *l* when the interacting nuclei undergo fusion.
- For given projectile energy (E) and potential, there is a value l_{crit} above which no fusion.

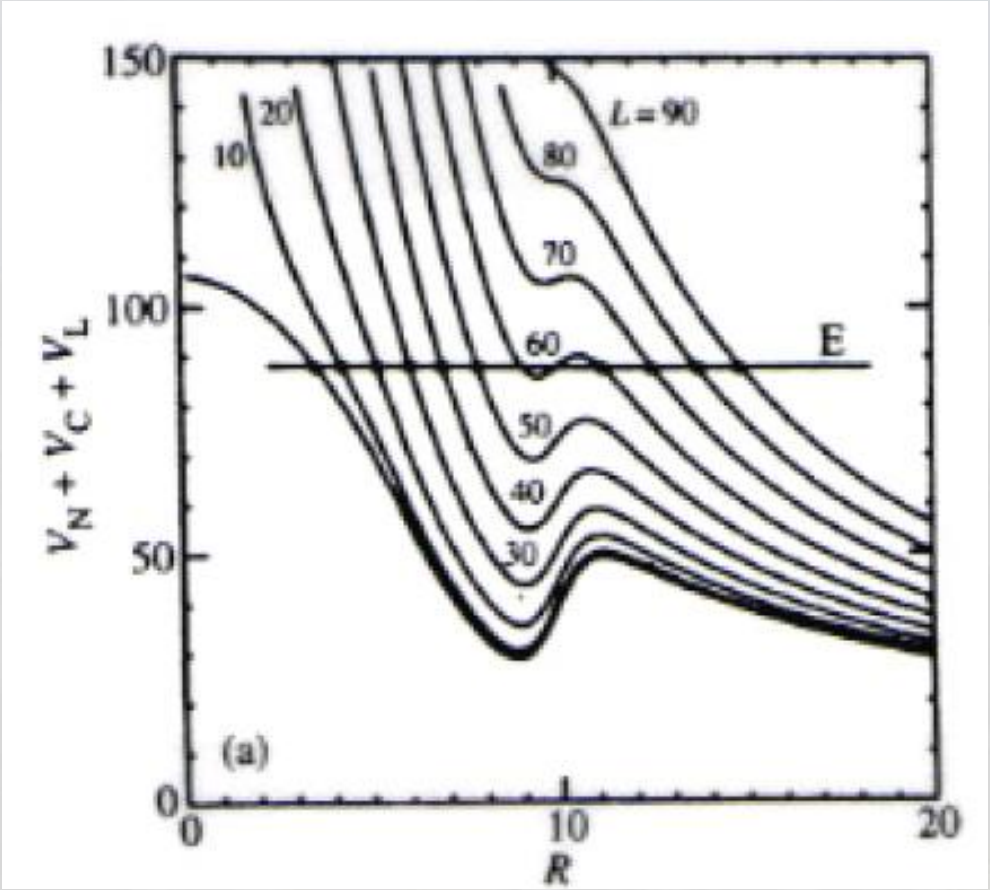

Source: *Loveland 2005*

Introduction (contd.)

^{208}Pb (^{50}Ti, xn) $^{258-x}Rf$ (x=1-3)

→ Superheavy element production (Z=104).

→ The probability that the mononuclear complex evolves to form a CN inside the fission saddle point (P_{CN}) is an important factor.

→Aimed at determining this probability experimentally for the given system.

→ Stable target and projectile combination.

^{9}Li + ^{70}Zn (and an attempt of ^{11}Li + ^{70}Zn)

→ Radioactive projectiles which have an interesting nuclear structure, neutron *skin* and *halo*.

→ Theoretical as well as experimental disagreement over the effect of these nuclear structures on fusion.

→ Presence of any suppression or enhancement of sub-barrier fusion as compared with the stable beams would be determined.

Oregon State UNIVERSITY OSU

Determination of P_{CN} in $^{50}Ti + ^{208}Pb$ fusion reaction

Oregon State UNIVERSITY OSU

Background and motivation

Nuclear reaction mechanisms

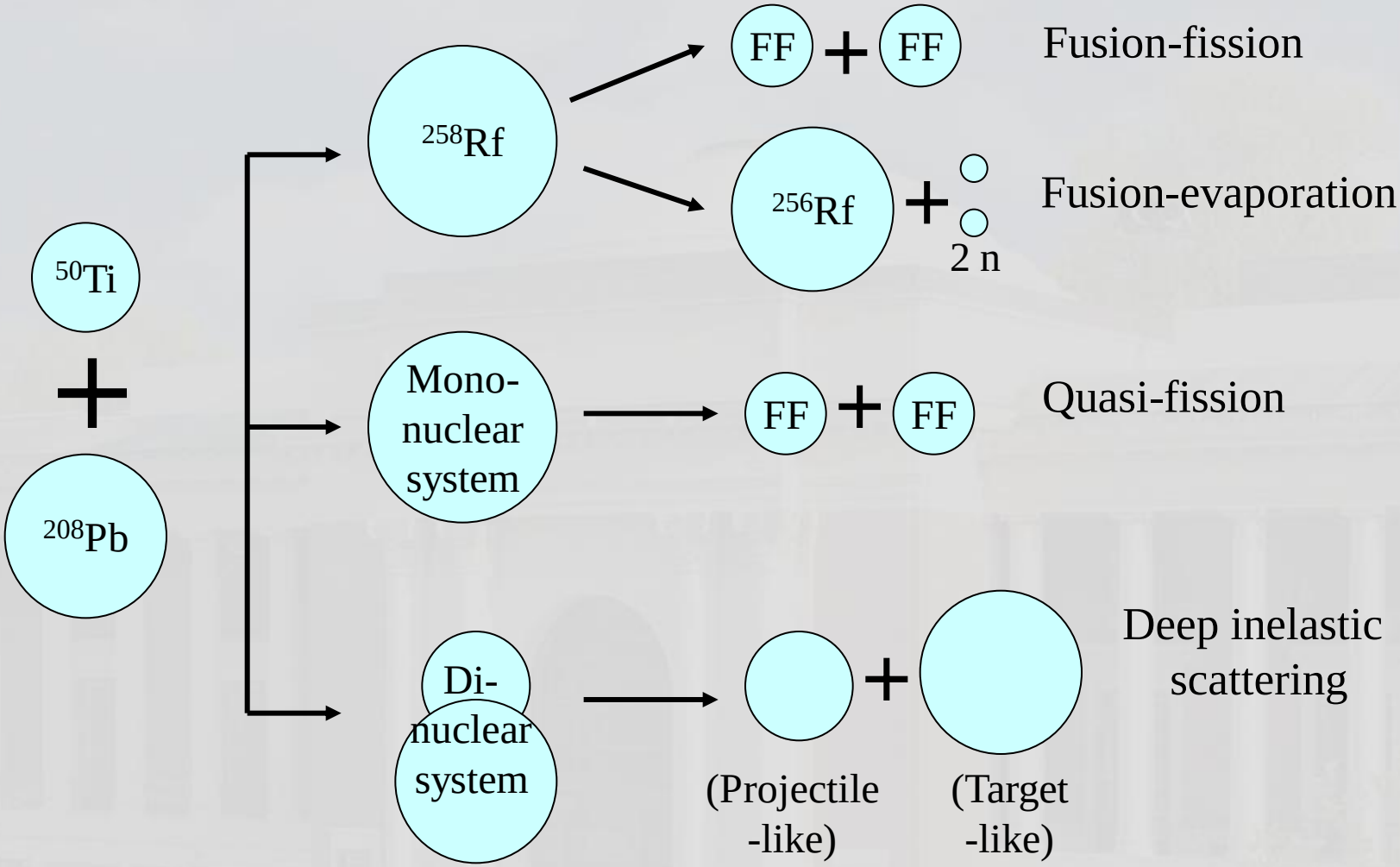

Production cross section

$$\sigma_{EVR} = \sigma_C * P_{CN} * W_{SUR}$$

Measured by Heßberger et al. *(Heßberger 1997)*

Measured by Clerc et al. *(Clerc 1984)*

Determined theoretically using methods given by Smolańczuk *(Smolańczuk 1995; Smolańczuk 1999)* and by Möller et al. *(Möller 1988; Möller 1995)*.

Theoretical calculation of W_{sur}

$$\frac{\Gamma_n\left(E^*_{CN}\right)}{\Gamma_f\left(E^*_{CN}\right)} = \frac{4A^{2/3}\left(E^*_{CN} - B_n\right)}{k\left(2\left[a\left(E^*_{CN} - B_f\right)\right]^{1/2} - 1\right)} \exp\left[2a^{1/2}\left(\left(E^*_{CN} - B_n\right)^{1/2} - \left(E^*_{CN} - B_f\right)^{1/2}\right)\right]$$

$$W_{sur}\left(E^*_{CN}, J\right) \approx P_{xn}\left(E^*_{CN}, J\right) \prod_{i=1}^{x} \frac{\Gamma_n\left((E^*_{CN})_i, (J)_i\right)}{\Gamma_n\left((E^*_{CN})_i, (J)_i\right) + \Gamma_f\left((E^*_{CN})_i, (J)_i\right)}$$

- Zubov et al. calculated Γ_n/Γ_f and W_{sur} *(Zubov 1999)* for 1n evaporation channel using the two theoretical predictions.
- Values differ by more than an order of magnitude, difference attributed to difference in B_f as the B_n values similar.
- For Z=104 (Rf),

Method	Γ_n/Γ_f	W_{sur}
Smolańczuk	2.0×10^{-2}	1.0×10^{-3}
Möller et al.	2.5×10^{-3}	1.2×10^{-4}

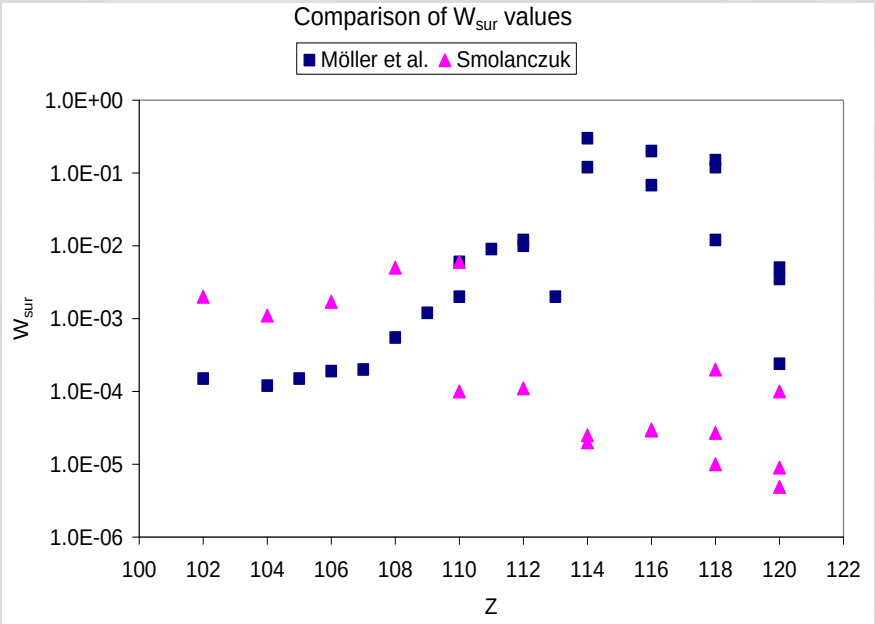

Experimental determination of W_{sur}

$$\sigma_{EVR} = \sigma_C * P_{CN} * W_{SUR}$$

Measured by Heßberger *(Heßberger 1997)*

Measured by Clerc et al *(Clerc 1984)*

Our aim is to find this quantity experimentally

Then calculate W_{SUR} and see which method it is closer to, Smolańczuk or Möller.

Oregon State UNIVERSITY OSU

Experimental details

Irradiation energy

•The data were acquired at five beam energies bracketing the maximum (238MeV) of the 2n EVR excitation function *(Heßberger 1997)*.

•At 230 and 233MeV, 1n evaporation channel is predominant with 230MeV being the maximum for it.

•The onset of 3n channel was expected at 243MeV with 253MeV being its maximum.

•Thus the data acquired spanned the 1n, 2n and 3n evaporation channels.

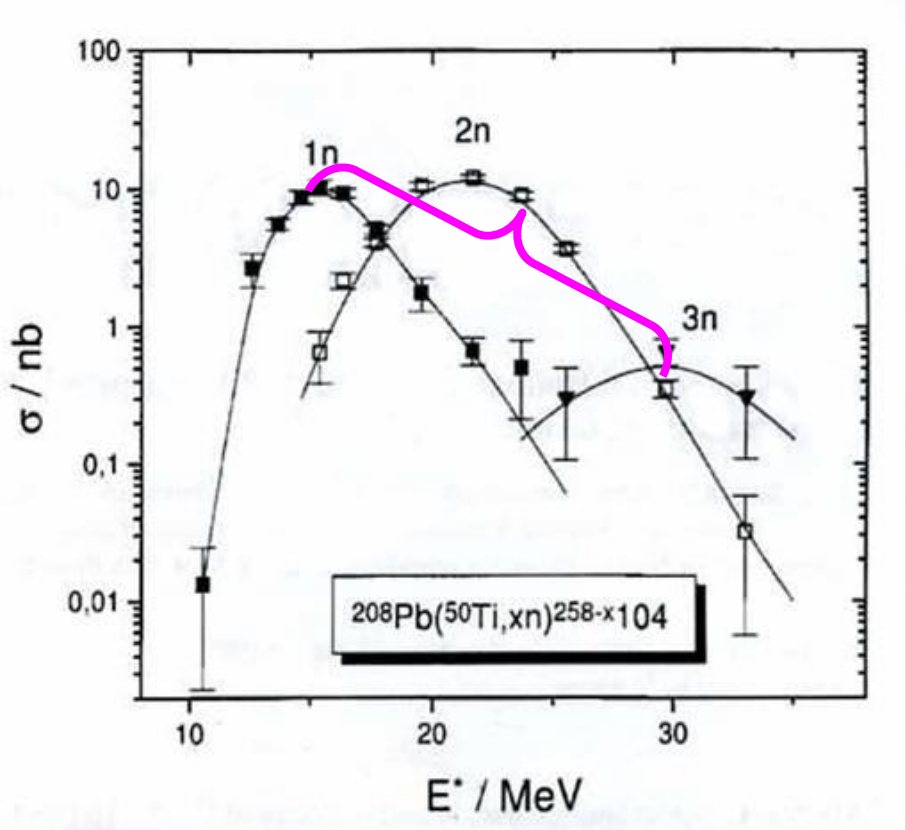

Source: *Heßberger 1997*

Experimental setup

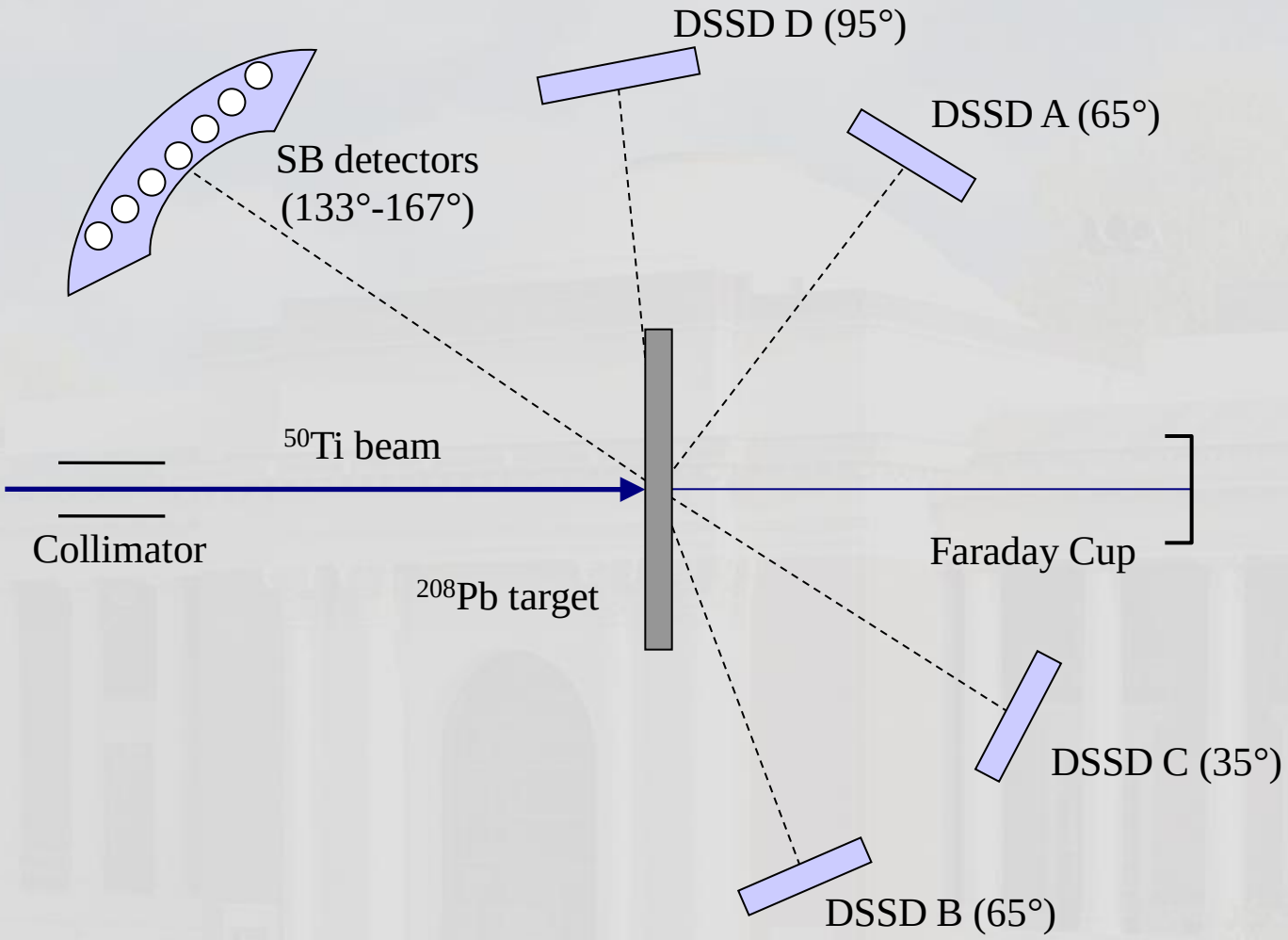

Data acquisition

•Before the experiment, energy spectra were recorded from ^{252}Cf spontaneous fission source and with ^{197}Au and ^{208}Pb targets in singles mode (independent of other detectors).

•The elastic peaks from ^{50}Ti+^{197}Au and ^{50}Ti+ ^{208}Pb (ranging 230-85MeV), the ^{252}Cf spontaneous fission peak (~185MeV) and the α-emission peak (~6MeV) would define the energy range for calibration.

•All further data collection was performed with coincidence mode (events recorded only when they occur simultaneously in two or more detectors) condition put on detectors A-B and C-D (separated by the ‘folding angle’ for this reaction (130°)). This data signified the occurrence of fission.

•There was no coincidence condition put on the array of SB detectors at the backward angles throughout the experiment.

Oregon State UNIVERSITY OSU

Data analysis and results

Energy calibration

For very heavily ionizing particles, the high density of electron-hole pairs created in a semiconductor detector leads to space-charge phenomena which affect the 'rise time' and 'pulse height' of the resulting signal.

→The electron-hole pairs nullify the local charge and rise time of pulse is longer than usual.
→During this delay, electrons and holes get recombined and the pulse height detected is smaller than actual.

This is the ***Pulse Height Defect*** (PHD) which results in detector calibration being different for different particle types.

Energy calibration (contd.)

To get rid of this defect, calibration is done using the Schmitt-Kiker-Williams (SKW) method *(Schmitt 1965)*. Coefficients are calculated for each detector or strip using the pulse heights of the ^{252}Cf SF source peaks as follows,

$$a = \frac{24.0203}{P_L - P_H} \qquad a' = \frac{0.03574}{P_L - P_H} \qquad b = 89.6083 - a \times P_L \qquad b' = 0.1370 - a' \times P_L$$

Using these four coefficients into the following equation one can find the energy of a fission fragment of known mass,

$$E_{(MeV)} = \left[a + \left(a' \times M_{(amu)}\right)\right] \times P + \left[b + \left(b' \times M_{(amu)}\right)\right]$$

For our data analysis we assumed symmetric fission (M = 129amu).

Energy calibration (contd.)

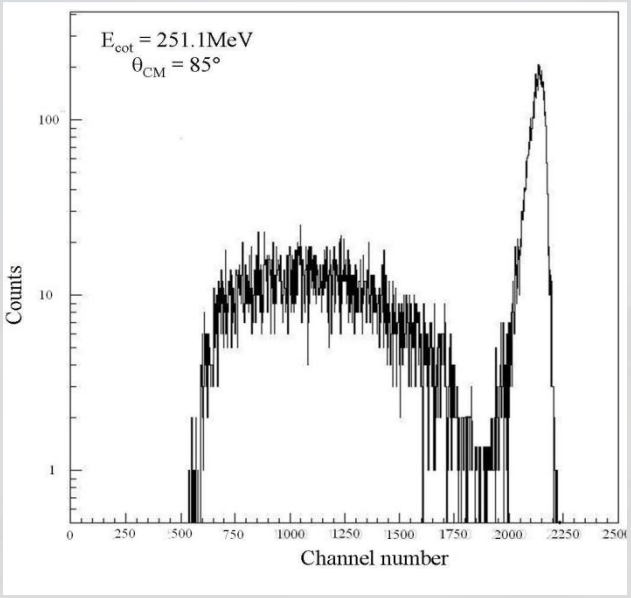

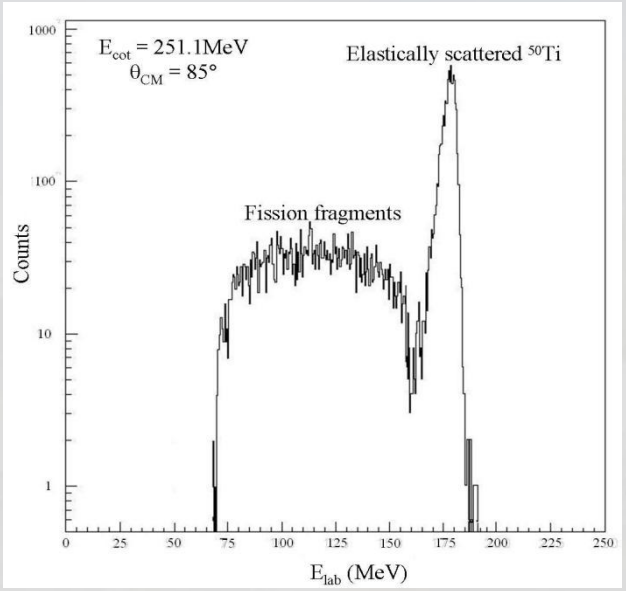

The energy loss in beam due to collisions with the target atoms needs to be taken into consideration for kinematical calculations and data analysis.

$$\frac{dE}{dx} \approx \frac{MZ^2}{E}$$

Beam	Target	Energy loss (MeV)
^{50}Ti	^{208}Pb	~2.0
^{50}Ti	^{197}Au	~1.0

Time calibration

Following formula was utilized to arrive at the expected time (nanoseconds, ns) at which the elastically scattered particles would reach a particular detector at a given beam energy,

$$t = (0.72) \times l \times \sqrt{\frac{A}{E}}$$

The straight line equations for each detector or strip were used to calibrate the timing spectra.

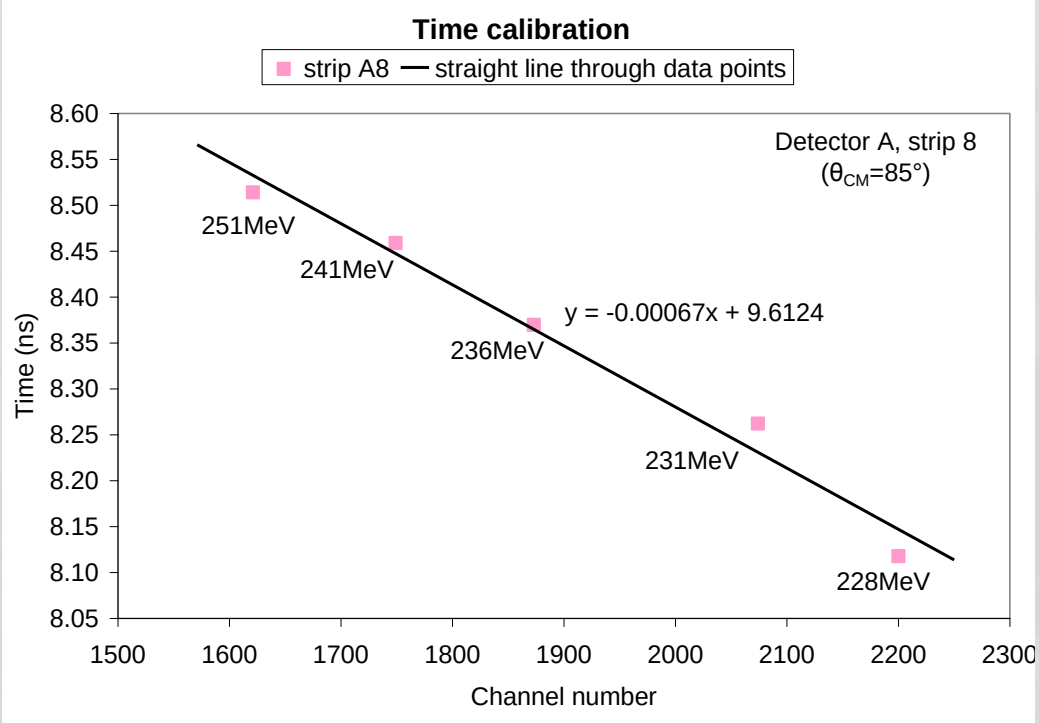

Time calibration (contd.)

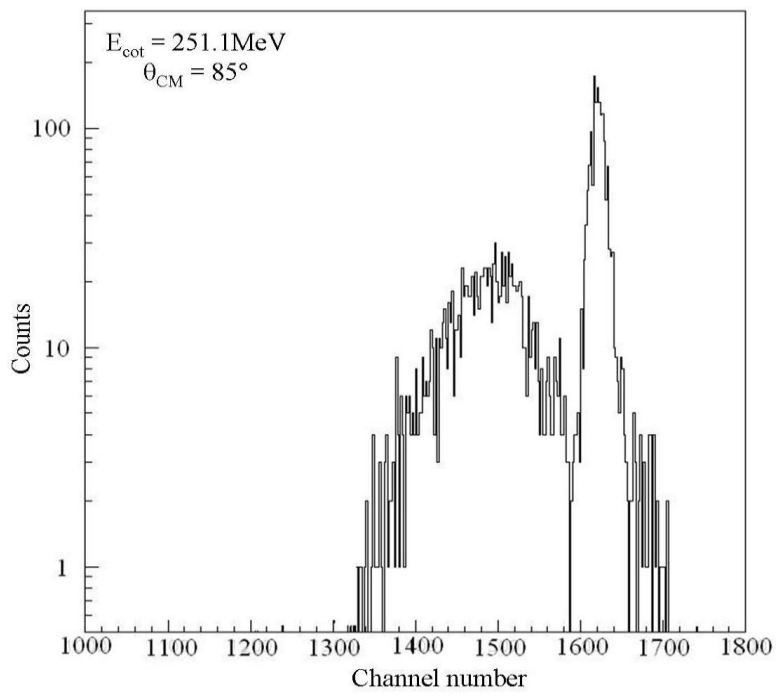

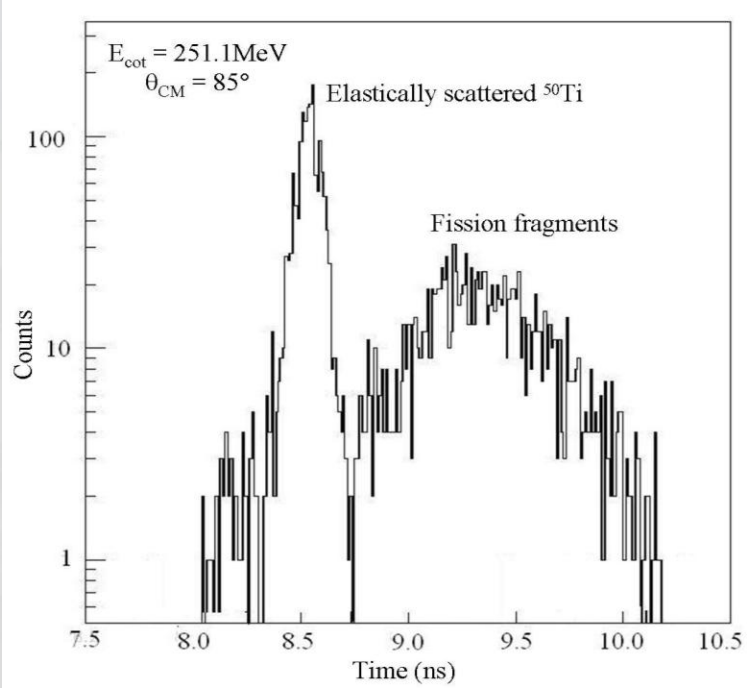

- The timing spectrum is recorded in reverse direction with the DAQ.
- Converted to the correct direction during calibration.

Cross section calculation

$$\frac{d\sigma}{d\Omega} = \frac{\#\,\text{fission events}}{(\#\,\text{target atoms})(\#\,\text{particles incident on target})(\text{Detector solid angle})}$$

$$\#\,\text{of target atoms} = \frac{\text{Weight of target material} \times N_A}{A_t}$$

$$\text{Integrated beam current (pnA)} = \frac{\text{Integrated beam current (enA)}}{\text{Charge on the particle}}$$

$$\#\,\text{of particles incident on target} = \text{pnA} \times (6.25 \times 10^9\ \text{particles/s}) \times \text{duration of run}$$

$$\text{Solid angle } (\Omega) = \frac{A}{r^2}$$

Cross section calculation (contd.)

•Data obtained in coincidence mode with the DSSD pair A-B.

•Recorded only the FFs resulting from fusion-fission reaction involving full-momentum transfer.

•Number of fission events detected by each pair of strips determined from the E_1 vs E_2 plots.

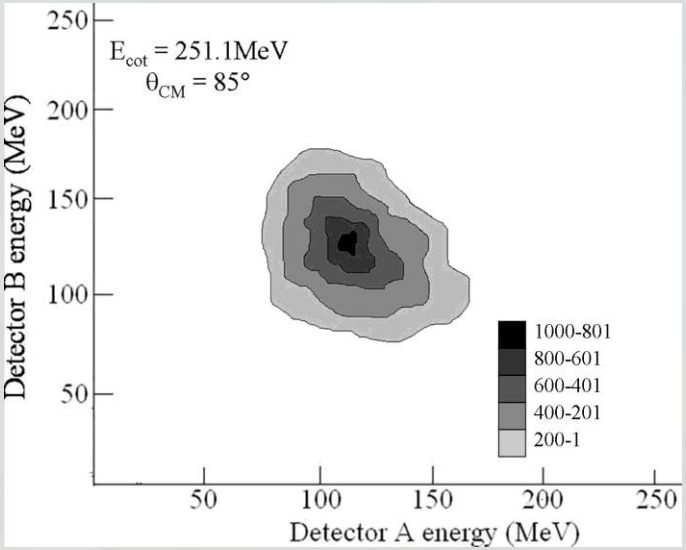

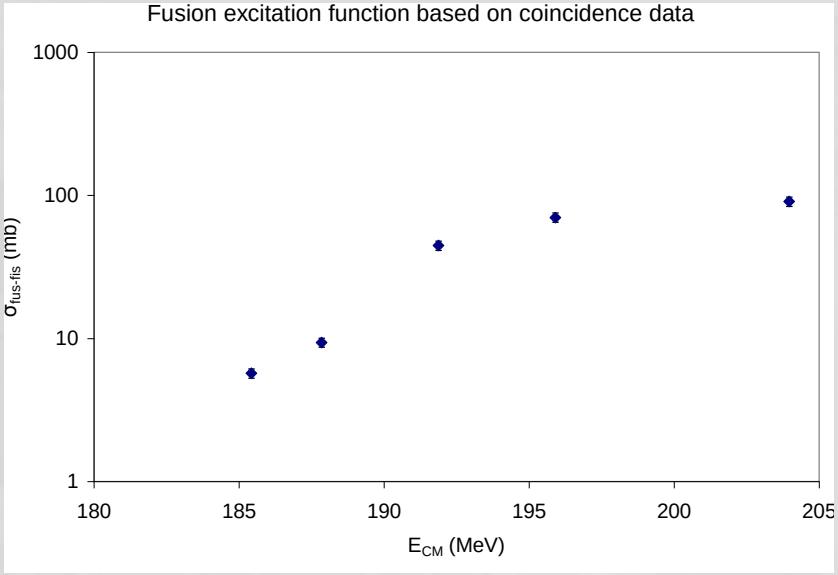

•Differential c.s. integrated over 4π to get the total $\sigma_{fus-fis}$ for each energy.

Cross section calculation (contd.)

•Data acquired in singles mode from the SB detectors.

•Number of fission fragments determined from the E vs A spectra which separated the reaction products based on their masses.

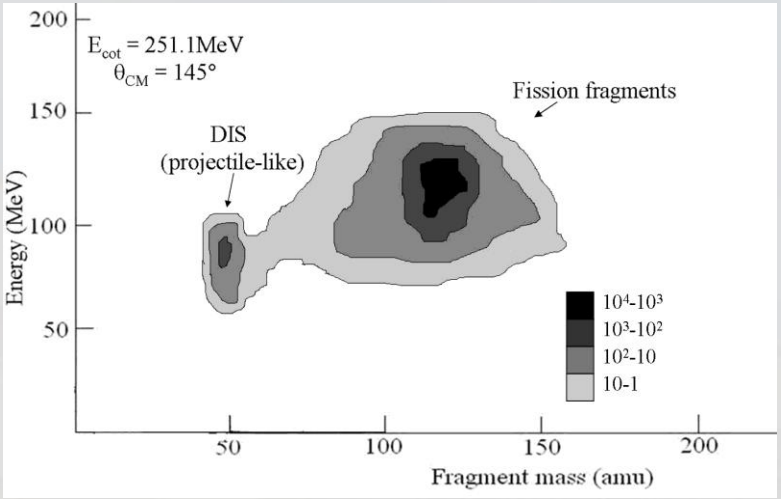

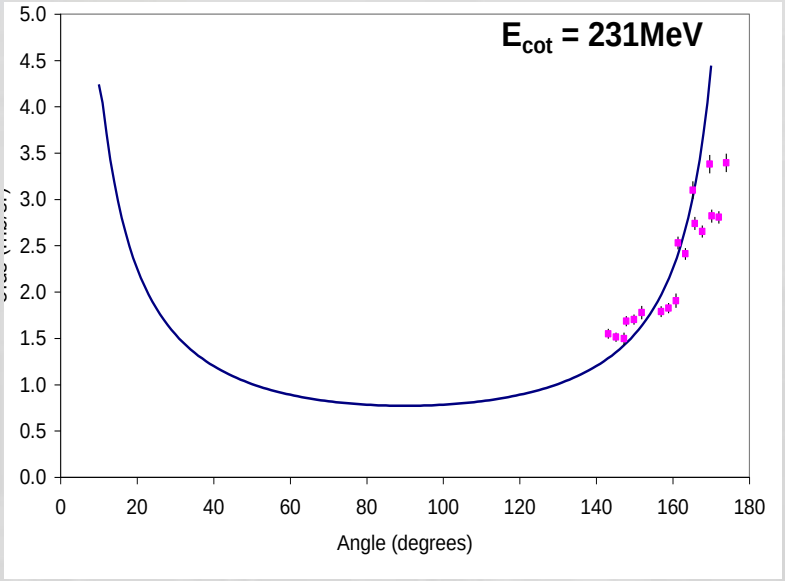

•FF emission is isotropic ($d\sigma_{fis}$ is constant as function of θ).

•$d\sigma_{fis}/d\Omega$ should follow the shape of $1/\sin\theta$ (as $d\Omega$ is proportional to $\sin\theta\, d\theta$).

•The angular distribution shows significant rise in $d\sigma_{fis}/d\Omega$ as expected for the detectors at backward angles.

Angular distribution fitting

•The FFs arise from the fusion-fission as well as quasi-fission. In order to determine the P_{CN} it was important to determine the relative contributions of compound nucleus formation and quasi-fission to the total fission cross section.

→The fusion-fission angular distribution is isotropic.

→The quasi-fission angular distribution is forward and backward peaking.

•Therefore, the angular distributions of SB detectors at backward angles were fit according to Back et al. *(Back 1985)* prescription, with the following function,

$$W(\theta) \propto \sum_{J=0}^{\infty} \frac{(2J+1)^2 T_J \exp\left[\frac{-\left(J+\frac{1}{2}\right)^2 \sin^2\theta}{4K_0^2}\right] J_0\left[\frac{i\left(J+\frac{1}{2}\right)^2 \sin^2\theta}{4K_0^2}\right]}{erf\left[\frac{\left(J+\frac{1}{2}\right)}{\left(2K_0^2\right)^{1/2}}\right]}$$

Angular distribution fitting (contd.)

•It was assumed that the cross section consisted of two components,

→ $J \leq J_{crit}$: compound nucleus formation

→ $J \geq J_{crit}$: quasi-fission.

$$J_{fis} = \left(\frac{\sigma_{fus-fis}}{\pi \lambda\!\!\!^{-2}} \right)^{1/2} - 1 \qquad \pi \lambda\!\!\!^{-2} = \pi \left(\frac{\hbar}{\sqrt{2mE_{CM}}} \right)^2 \qquad K_0^{\,2} = \frac{T\ Ieff}{\hbar^2}$$

•These fits were integrated over 4π to arrive at σ_{fis}.

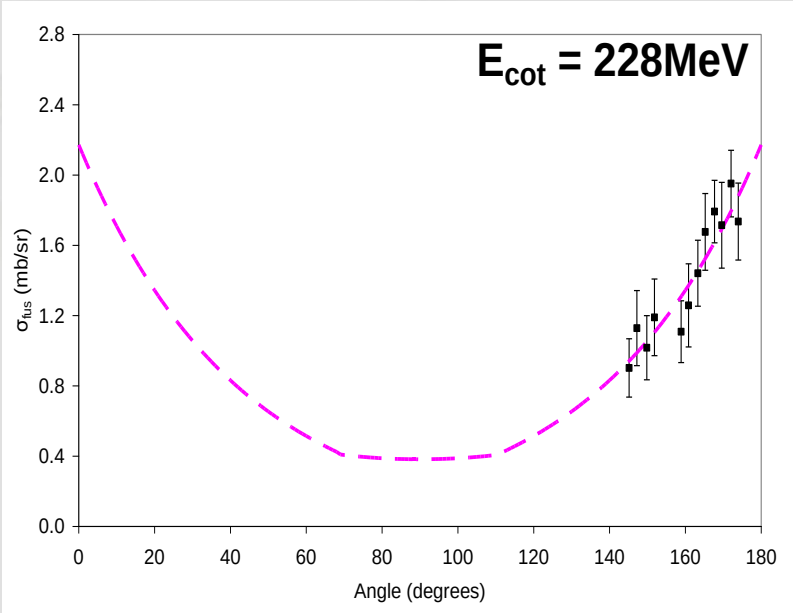

•From the J_{fis}, J_{crit} (=J_{CN}) and σ_{fis} values the relative contribution of complete fusion was determined as *(Back 1985)*,

$$\frac{\sigma_{CN}}{\sigma_{fis}} = \frac{J_{CN}^2}{J_{fis}^2} = P_{CN}$$

Cross sections σ_{fis} and σ_{CN}

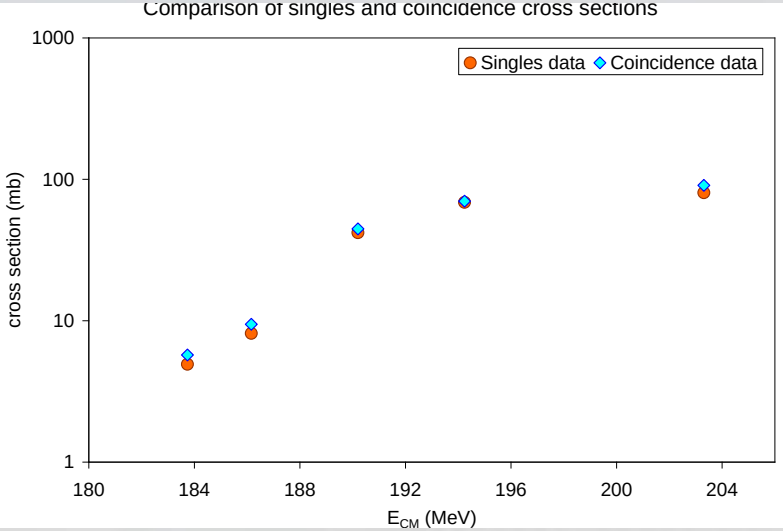

The cross sections calculated based on singles data from the SB detectors and those based on coincidence data from the DSSDs agree well with each other.

E_{cot} (MeV)	J_{fis} (ħ)	σ_{fis} (mb)	Degrees of freedom	Reduced χ^2	J_{CN} (ħ)	σ_{CN} (mb)
228.0	7	5.72±0.57	11	1.82	1	0.11±0.02
231.0	9	8.39±0.91	17	2.37	2	0.40±0.06
236.0	22	43.30±1.90	23	2.60	10	9.82±1.07
241.0	28	69.40±0.90	5	0.14	12	12.75±1.28
251.1	32	85.50±7.30	23	0.35	15	18.78±2.50

P_{CN} and W_{sur}

- σ_{EVR} determined from EVR excitation functions measured by Hoffman et al. *(Hoffman 2004)*, an improvement over Heßberger et al. measurement.
- σ_c ($=\sigma_{fis}$) and P_{CN} (σ_{CN}/σ_c) measured in this work.

E_{CM} (MeV)	σ_{EVR} (mbarns)	σ_c (mbarns)
183.74	$1.3\times10^{-5}\pm2.0\times10^{-6}$	5.72±0.57
186.16	$1.6\times10^{-5}\pm2.0\times10^{-6}$	8.39±0.91
190.20	$1.7\times10^{-5}\pm2.0\times10^{-6}$	43.30±1.90
194.24	$6.0\times10^{-6}\pm2.0\times10^{-6}$	69.40±0.90
203.31	$1.0\times10^{-6}\pm1.0\times10^{-7}$	85.50±7.30

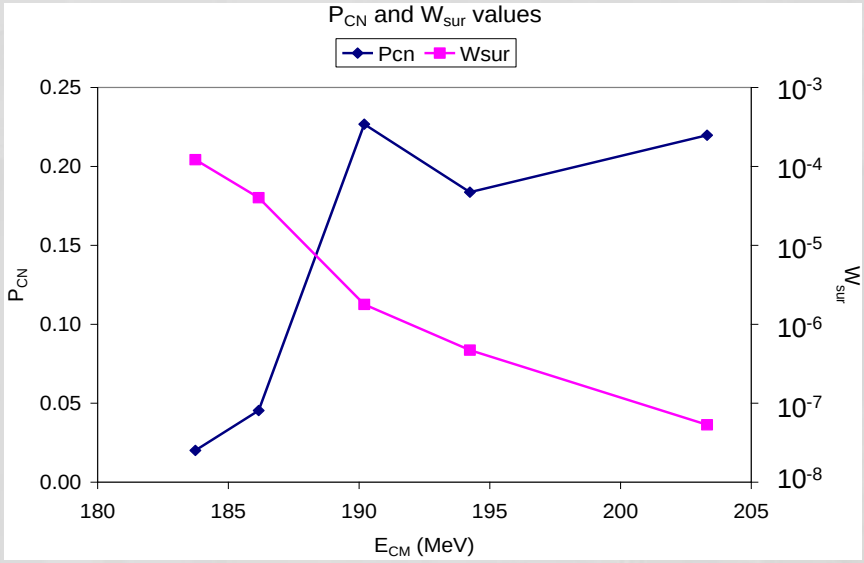

Comparison

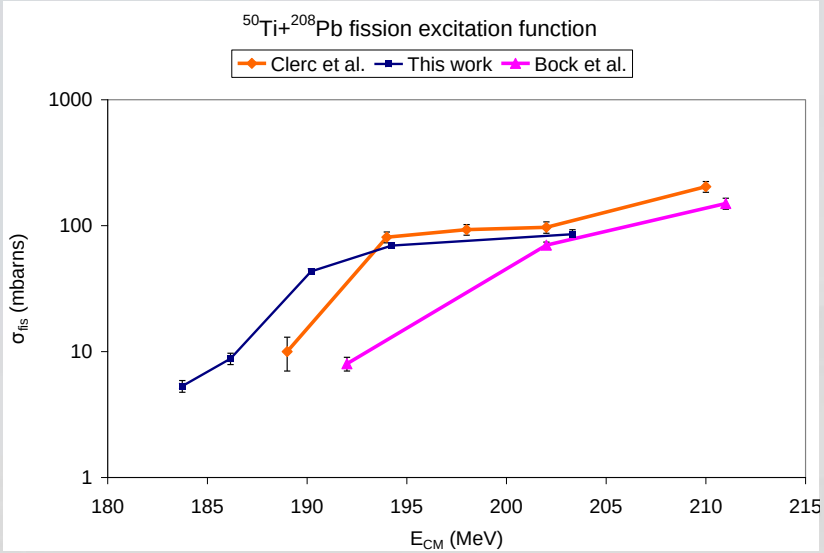

- The σ_c is in fair agreement with the ones measured by Clerc et al. *(Clerc 1984)*.
- Those obtained by Bock et al. *(Bock 1982)* are lower.

- Theoretically predicted $P_{CN} = 0.07$ *(Adamian 2000)*, "empirical" $P_{CN} = 0.01$ *(Siwek-Wilczynska 2005)* for ^{208}Pb (^{50}Ti, 2n) ^{256}Rf.
- Experimentally determined $P_{CN} = 0.23$ at $E^* = 20.6$MeV, max of 2n channel.

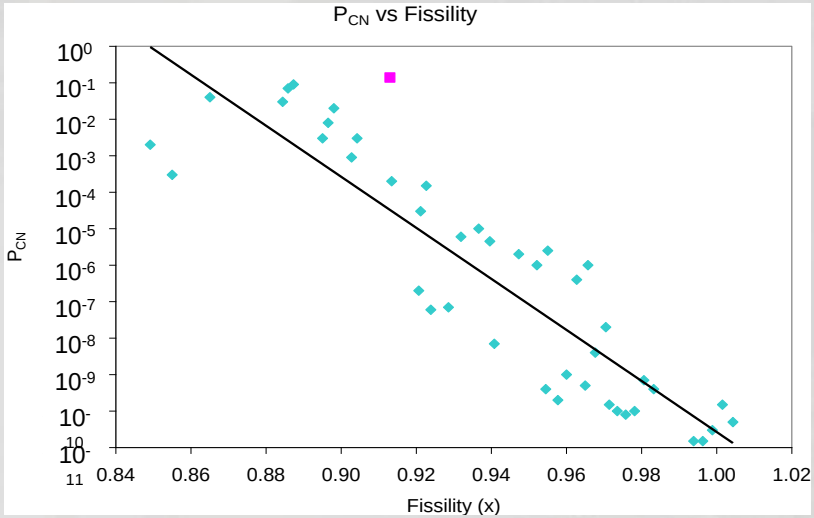

W_{sur}: experiment and theory

- W_{sur} values have been calculated for 1n channel by Zubov et al. *(Zubov 1999)* by using two different calculation schemes.

- Experimental $W_{sur} = 1.22 \times 10^{-4}$ for E* = 14.16MeV, maximum of 1n EVR excitation function; that obtained by Möller et al. prescription is 1.2×10^{-4}.

- Next two energies, combination of 1n and 2n decay modes causes the W_{sur} to decrease by just over an order of magnitude.

- Further decrease caused by onset of 3n decay channel for the last two energies.

- Theoretical values for comparison with the W_{sur} for 2n and 3n channels are, however, not available at this point.
- Zubov et al. mention the possibility of higher differences in W_{sur} for higher xn evaporation channels ($x \geq 2$). Only those calculations of W_{sur} should be of interest where a large enough number of reactions are considered within the same set of parameters and assumptions.

Future work

Is there a trend?

•Experiments need to be carried out in future for the systems that would produce CN with Z > 104 to find out the whether there is a trend of agreement with predictions of Möller et al. for heavier nuclei.

Oregon State UNIVERSITY OSU

Sub-barrier fusion of ^{9}Li with ^{70}Zn

(With an attempt to study ^{11}Li fusion with ^{70}Zn)

Oregon State UNIVERSITY OSU

Background and motivation

'Halo' and 'Skin' nuclei

- When nuclear force is effective in keeping the nucleus together, density of nucleons is uniform throughout the nucleus.
- Nucleons in very n-rich nuclei are not uniformly distributed, some nucleons are placed outside the bulk of nuclear matter, at a radius much larger than $R_0 x A^{1/3}$.
- Feel attractive nuclear force less strongly, form a 'halo' around the core (nucleons within the predicted nuclear radius).
- Nuclei with this structure are called 'halo nuclei'. e.g. ^{11}Li (abnormally spatially extended *(Tanihata 1985)* with matter radius 3.27± 0.24 fm as compared to 2.7fm predicted by $R_0 x A^{1/3}$).
- Few other nuclei with very similar characteristics but not as spatially extended as the halo nuclei, the detached nucleons around them are called 'skin'. e.g. ^{9}Li.

Theoretical contradictions

•Near or sub-barrier enhancement due to lower Coulomb barrier and Soft Dipole Mode *(Takigawa 1993)*.

•Sub-barrier lowering due to breakup and slight enhancement above barrier *(Hussein 1995)*.

•Breakup will not necessarily lead to lowering of σ_{fus} *(Dasso 1994)*.

The 'soft dipole mode' is a low energy branch (with excitation energy < 1MeV) of the 'giant dipole resonance'. GDR represents the oscillation of all the protons in a nucleus against the neutrons in it and the SDM symbolizes the halo neutrons oscillating against the core.

Experimental contradictions

- ^{6}He
  - →Sub-barrier enhancement *(Penionzhkevich 1995; Kolata 1998; Trotta 2000; Penionzhkevich 2006)*
  - →No enhancement *(Raabe 2004; Di Pietro 2004)*
- ^{11}Be
  - →Above barrier enhancement *(Signorini 1998)*
  - →No enhancement *(Yoshida 1995)*
- ^{9}Be
  - →No lowering near or above barrier *(Moraes 2000)*
  - →No lowering sub-barrier *(Cujec 1979; Mukherjee 1997)*
  - →Lowering near or above barrier *(Eck 1980; Figueira 1993; Dasgupta 1999)*
- ^{6}Li
  - →Sub-barrier enhancement *(Mukherjee 2001; Beck 2003)*
- ^{7}Li
  - →Above barrier lowering *(Tripathi 2002)*
  - →Sub-barrier enhancement *(Mukherjee 2001; Tripathi 2002)*

Reasons for studying $^{9}Li + ^{70}Zn$ system

- Insight into the nuclear structure of a very n-rich skin nucleus and mechanism for interaction with n-rich target.
- ^{11}Li nucleus = ^{9}Li core + 2n halo, would facilitate the understanding of ^{11}Li nuclear structure.
- Nuclear structure of ^{9}Li well-understood using the simple shell model, modeling reactions easy.
- Fusion studies have been performed by comparing the n-evaporation spectra with theoretical predictions but σ_{fus} was not measured.
- Product nuclei, Ge or As isotopes, can be separated by solvent extraction and can be detected by γ and β spectroscopy.
- Availability of the maximum ^{9}Li beam energy 15.4MeV at the ISAC1 facility, it was possible to overcome fusion barrier.
- ^{70}Zn is medium mass nucleus with no special nuclear structure effects.

Reasons for studying $^{11}Li + ^{70}Zn$ system

- Pilot study, ^{11}Li along with ^{9}Li would allow a comparative study of skin and halo nuclei.
- Theoretical and experimental contradictions regarding the effect of nuclear halo structure on fusion need to be settled.
- Product nuclei, Ge or As isotopes, can be separated by solvent extraction and can be detected by γ spectroscopy.
- Availability of the maximum ^{11}Li beam energy 17.5MeV at the ISAC1 facility, it was possible to overcome fusion barrier.

Oregon State UNIVERSITY OSU

Experimental details

Zn targets

- Targets 1mg/cm^2 (diameter = 1.9 cm) on Al foil (0.54-0.71mg/cm^2).
- Electrolyte
  - →1760mg $ZnSO_4.7H_2O$
  - →220mg $Al_2(SO_4)_3.18H_2O$
  - →110mg NH_4Cl
  - →100ml deionized water.
- 1mA current for 20 minutes, continuous stirring.
- Maintained at pH 3-4.
- For ^{70}Zn targets, ^{70}ZnO was dissolved in H_2SO_4 to obtain $^{70}ZnSO_4$.

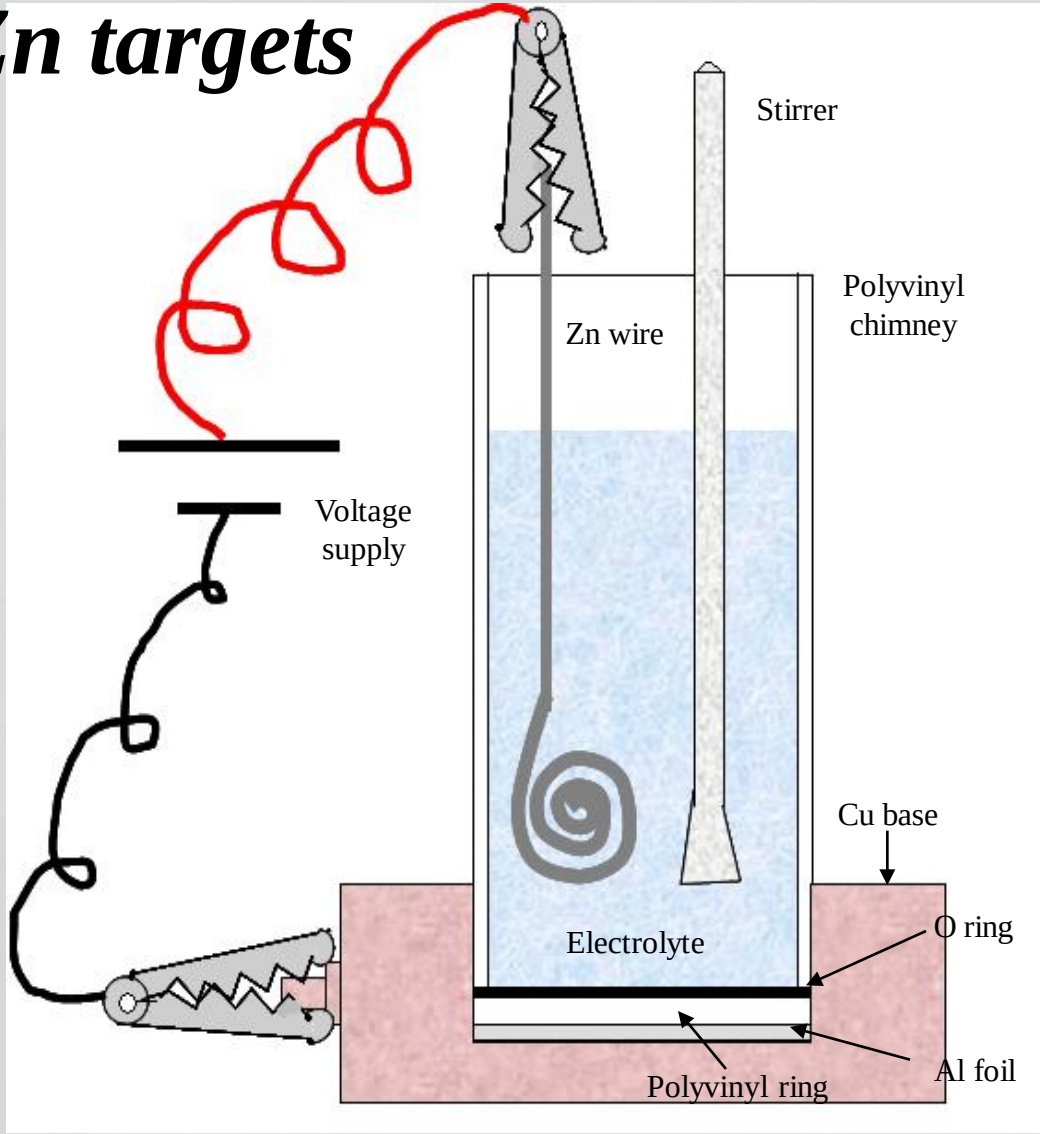

Solvent Extraction

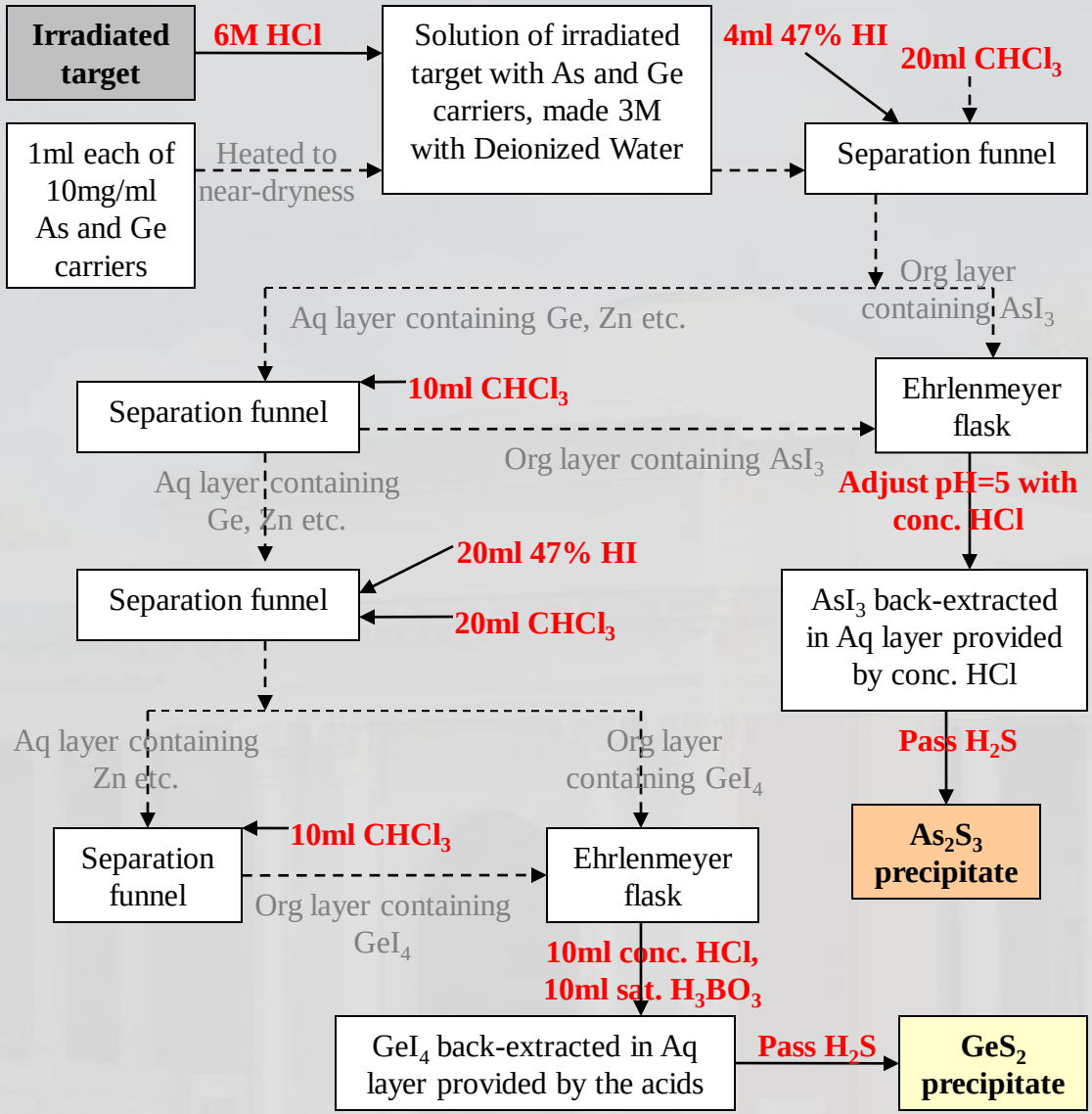

Delayed neutrons protective shield

- ^{9}Li :178ms *(Alburger 1976)* β emitter, Q_{β} ~13.6MeV *(Ajzenberg-Selove 1979)*.
  : ~50% decays resulting in delayed n-emission.
- Shield of 5% boron-loaded paraffin as protection.

- Paraffin: Alkane hydrocarbons, C_nH_{2n+2}, $n \geq 20$.
  - Amount: H atoms ~67%, Borax added such that B ~5%.
  - Hydrogen: Effective 'moderator', mass almost the same as neutron, neutrons scattered until they have become thermal neutrons.
  - Boron: Absorbs thermalized neutrons effectively (σ = 5mb for ^{11}B).

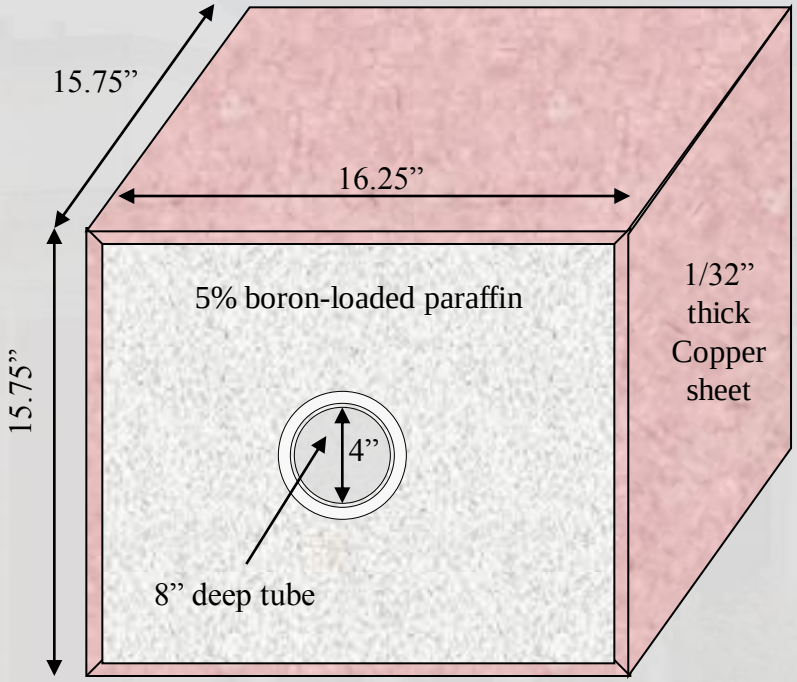

Experimental setup

•Experimental chamber inner diameter 20in.

•Faraday cup at 25in downstream from the center.

•300mm^2 SB detector mounted at about 40cm from the target at angle of 16.2°.

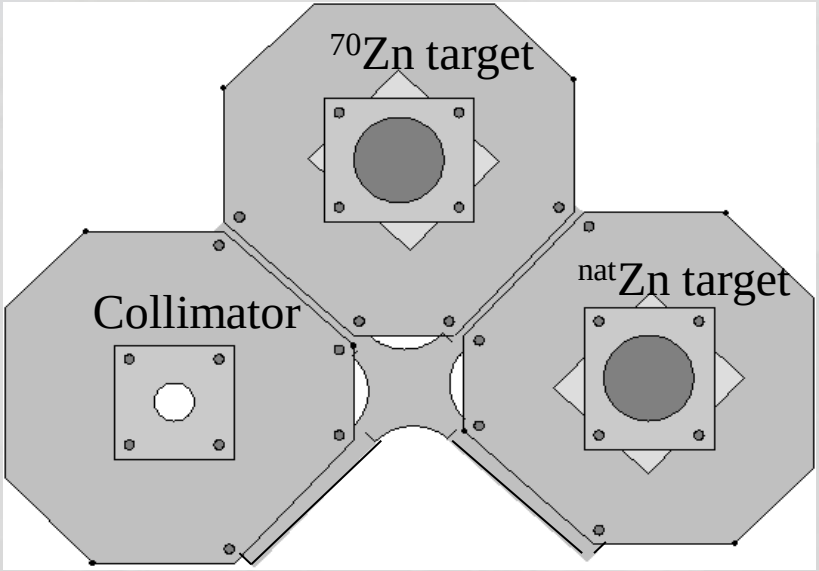

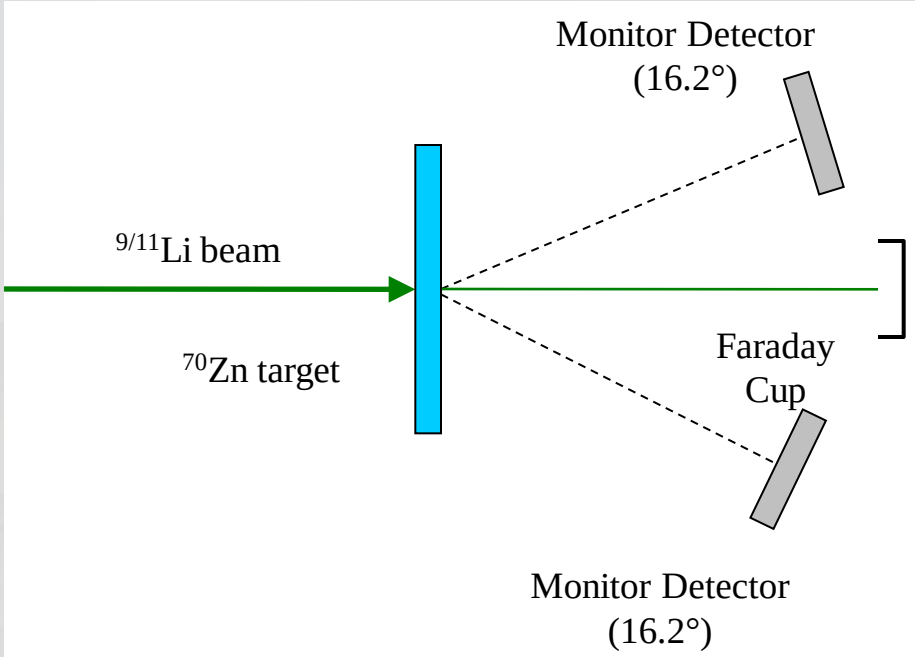

•Target wheel was 6in upstream from the center, target flaps mounted such that targets perpendicular to beam.

•A port in the bottom of the chamber used for evacuating it to ~5x10^{-6} Torr.

Irradiation, separation and counting

- Experiment carried out at seven different energies of ^{9}Li beam.

- New ^{70}Zn target was mounted for each energy and was irradiated for 1-3 days.

- After irradiation, target was counted in γ counter for about a day (in the 2006 attempt) and subjected to radiochemical separation subsequently.

- In the 2005 attempt low beam doses produced low activity in the target difficult to discern in the γ spectroscopy. The targets were, therefore, subjected directly to radiochemical separation.

- The separated precipitates were monitored for activity via β counting.

Oregon State UNIVERSITY OSU

Data analysis and results

Beam dose

- Beam dose monitored by detecting the elastically scattered beam.
- Two monitor detectors at ±16.2° with respect to the beam.

Nuclide	E_{lab} (MeV)	Target thickness (mg/cm^2)	Energy loss (MeV)	E_{cot} (MeV)	Beam dose (particles)	Average beam intensity (particles/s)
^{9}Li	15.4	0.89	0.4	15.0	3.08×10^{11}	8.45×10^{6}
	15.4	1.21	0.5	14.9	5.35×10^{11}	5.35×10^{6}
	15.1	1.02	0.4	14.7	4.16×10^{11}	3.38×10^{6}
	14.5	1.06	0.4	14.1	5.87×10^{11}	3.80×10^{6}
	14.0	0.85	0.4	13.6	5.76×10^{11}	4.00×10^{6}
	13.5	1.28	0.5	13.0	2.29×10^{11}	3.80×10^{6}
	12.5	1.06	0.5	12.0	1.07×10^{12}	3.51×10^{6}
	11.5	1.07	0.5	11.0	3.41×10^{11}	6.71×10^{6}

β counter efficiency

- ^{14}C, ^{36}Cl, ^{90}Sr, ^{99}Tc and ^{147}Pm calibrated β sources with $E_{max\beta}$ spread over 0.156-0.709MeV were used.
- $E_{max\beta}$ of ^{76}As is 2.97MeV, efficiency determined by extrapolation to be 6.6%.

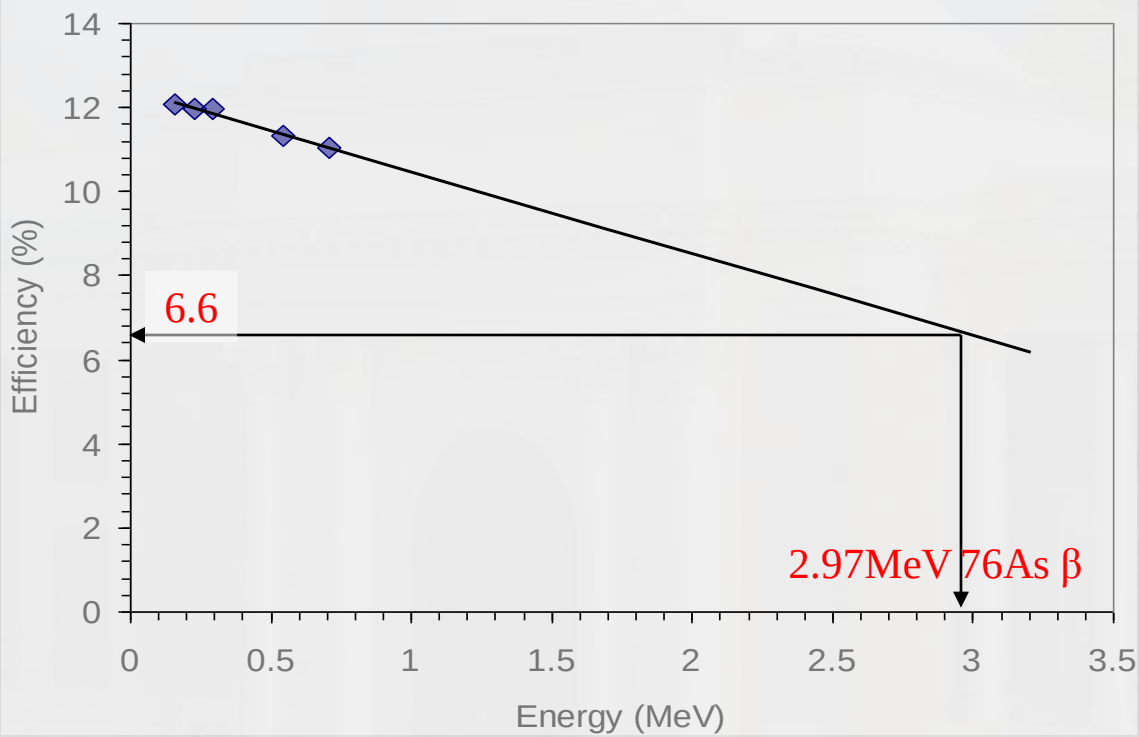

γ counter efficiency

- Calibrated γ sources ^{60}Co (1.17 and 1.33MeV),^{137}Cs (0.66MeV) and ^{152}Eu (0.12, 0.24, 0.34, 0.44, 0.78, 0.87, 0.11, 0.13 and 0.14MeV) were used.
- 2.0% efficiency for 559keV γ line emitted by ^{76}As.

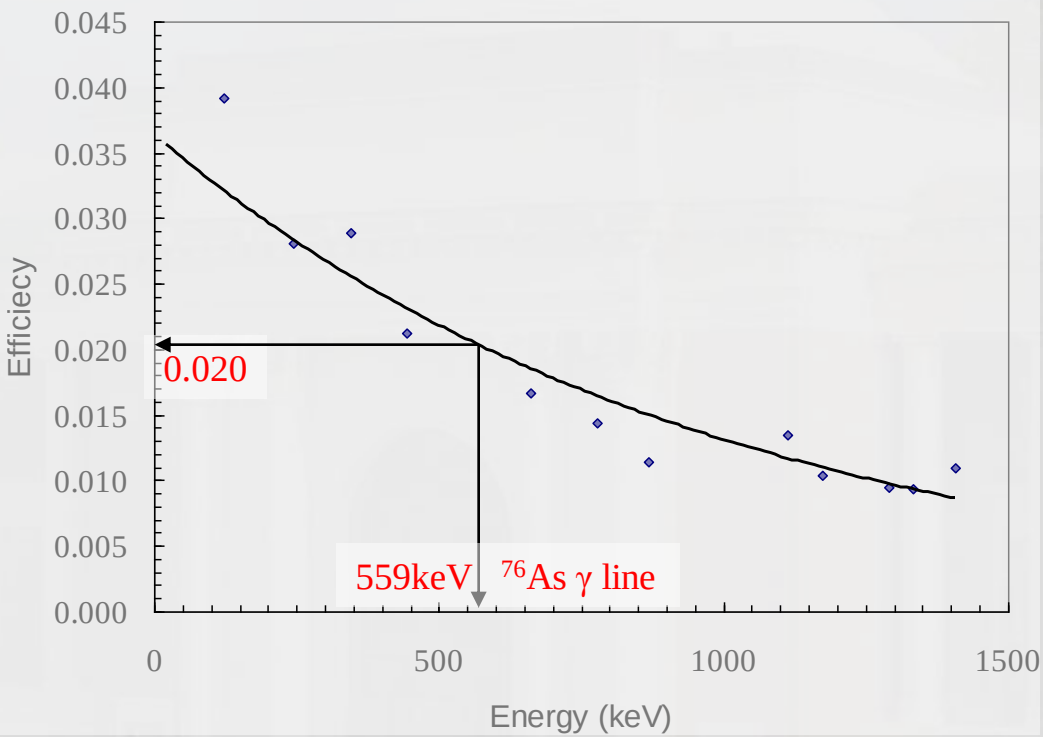

Isotopic purity and chemical yields

- Isotopic purity of ^{70}Zn targets
  - →Determined by carrying out a neutron activation analysis.
  - →Composition was 80.58% ^{70}Zn, 19.42% other isotopes of Zn (predominantly ^{64}Zn, 1115keV γ-line).

- Percent chemical yields for As and Ge precipitates
  - →Calculated by neutron activation along with 1ml standard As and Ge carriers.
  - →Yields ranged 27-100% (average = 63%) for As and 3-32% (average = 22%) for Ge.
  - →Reasons for low GeS_2 yields
    - Tendency to undergo incomplete precipitation in acidic medium.
    - Formation of colloidal precipitate which is difficult to filter.

Beta counting data analysis

- Activity in each As and Ge precipitate was followed for several days.
- Activity recorded at 100min intervals and plotted versus time to obtain decay curve for establishing the identity of isotopes present.

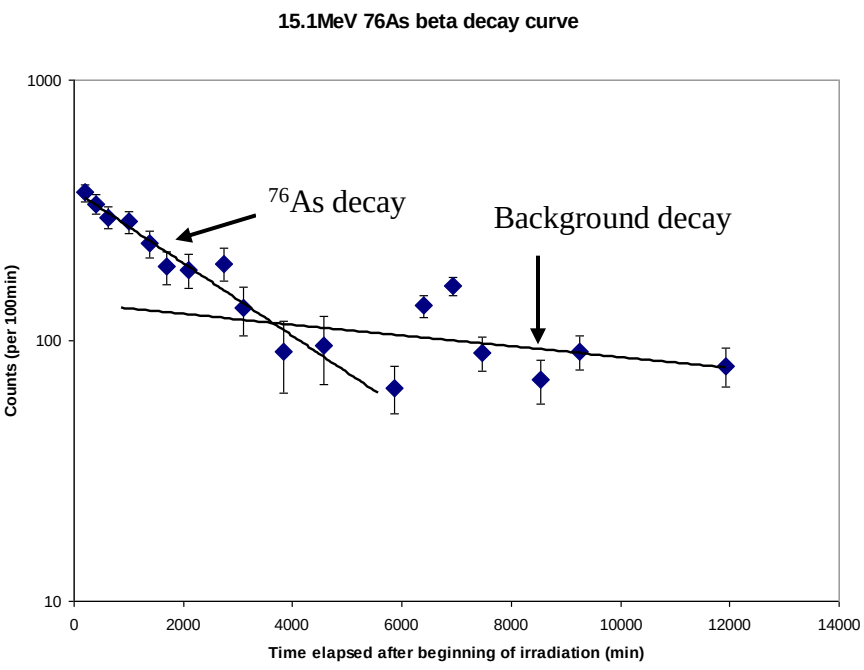

- Data resolved using DECHAOS software which fitted the data, gave $t_{1/2}$ and absolute activity at EOB (A_0)with percent error.
- These values and beam dose (φ) were processed through 'CROSS.for' to output σ_{prod} with the appropriate corrections applied.

$$\sigma = \frac{A_0 \times 10^{27}}{\phi \times N_t}$$

Beta counting data analysis (contd.)

- Counting done with As_2S_3 precipitates on filter papers. For such samples 'self-absorption correction' is needed.
- Some of the β emissions tend to get absorbed in the precipitate.
- Correction factors applied to our data ranged 0.85-0.99.

E_{lab} (MeV)	As_2S_3 precipitate thickness (mg/cm^2)	Self-absorption correction
15.4	6.35	0.987
15.1	5.03	0.990
14.5	8.07	0.980
14.0	8.07	0.980
13.5	17.98	0.909
12.5	9.69	0.978
11.5	16.87	0.920

Gamma counting data analysis

•Analysis was performed only for the data taken at 14.0, 14.5 and 15.1MeV ^{9}Li beams.

•'Handanal.for' read in the ASCII γ spectra and gave the peak areas and uncertainties.

$$\text{Absolute area of peak} = \text{Area of peak} - \text{Background}$$

$$\text{Uncertainty} = \sqrt{\text{Absolute area of peak} + \text{Background}}$$

•Data resolved using DECHAOS software which fitted the data, gave $t_{1/2}$ and absolute activity at EOB (A_0)with percent error.

•These values and beam dose (φ) were processed through 'CROSS.for' to output σ_{prod} with the appropriate corrections applied.

σ_{fus} calculation

•Fusion cross section (σ_{fus}) was obtained by correcting σ_{prod} for unobserved fusion products. Correction factor was taken as the average of the two ratios given below, values of which ranged between 0.72-0.83,

$$\left(\sigma_{fus}\right) \text{as computed by PACE 4.13} \Big/ \left(\sigma^{76}As\right) \text{as computed by PACE 4.13}$$

$$\left(\sigma_{fus}\right) \text{as computed by HIVAP} \Big/ \left(\sigma^{76}As\right) \text{as computed by HIVAP}$$

Projectile	E_{lab} (MeV)	Analysis method	σ_{fus}-γ (mb)	σ_{fus}-β (mb)
^{9}Li	11.5	β	-	30.0±5.8
	12.5	β	-	45.4±20.4
	13.5	β	-	69.6±10.7
	14.0	γ, β	205.5±19.5	167.3±28.0
	14.5	γ, β	285.8±20.1	202.2±26.2
	15.1	γ, β	421.8±26.3	302.7±20.4
	15.4	β	-	299.8±31.9

Cross sections based on β and γ data

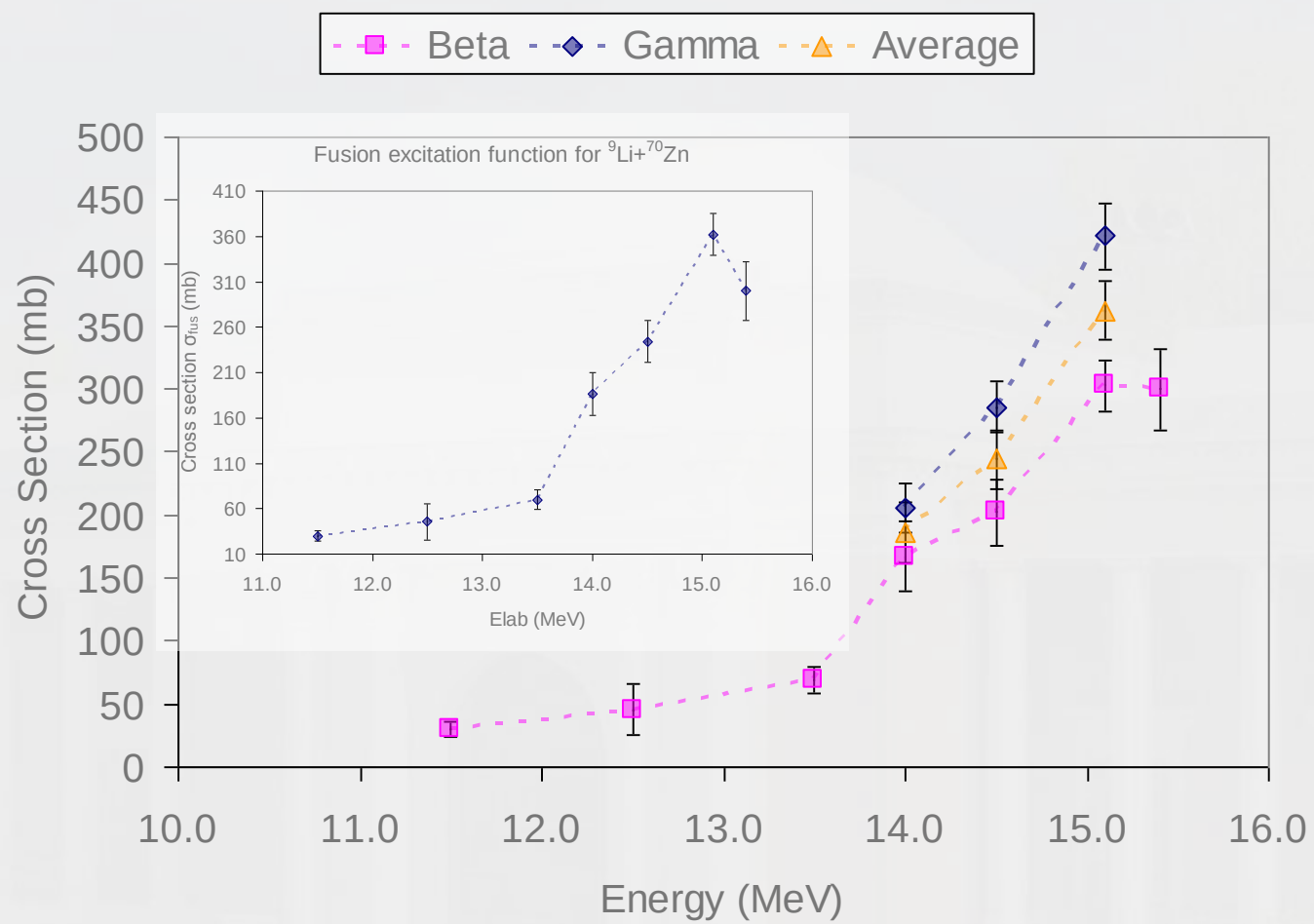

Oregon State UNIVERSITY OSU

Comparison of reduced excitation functions

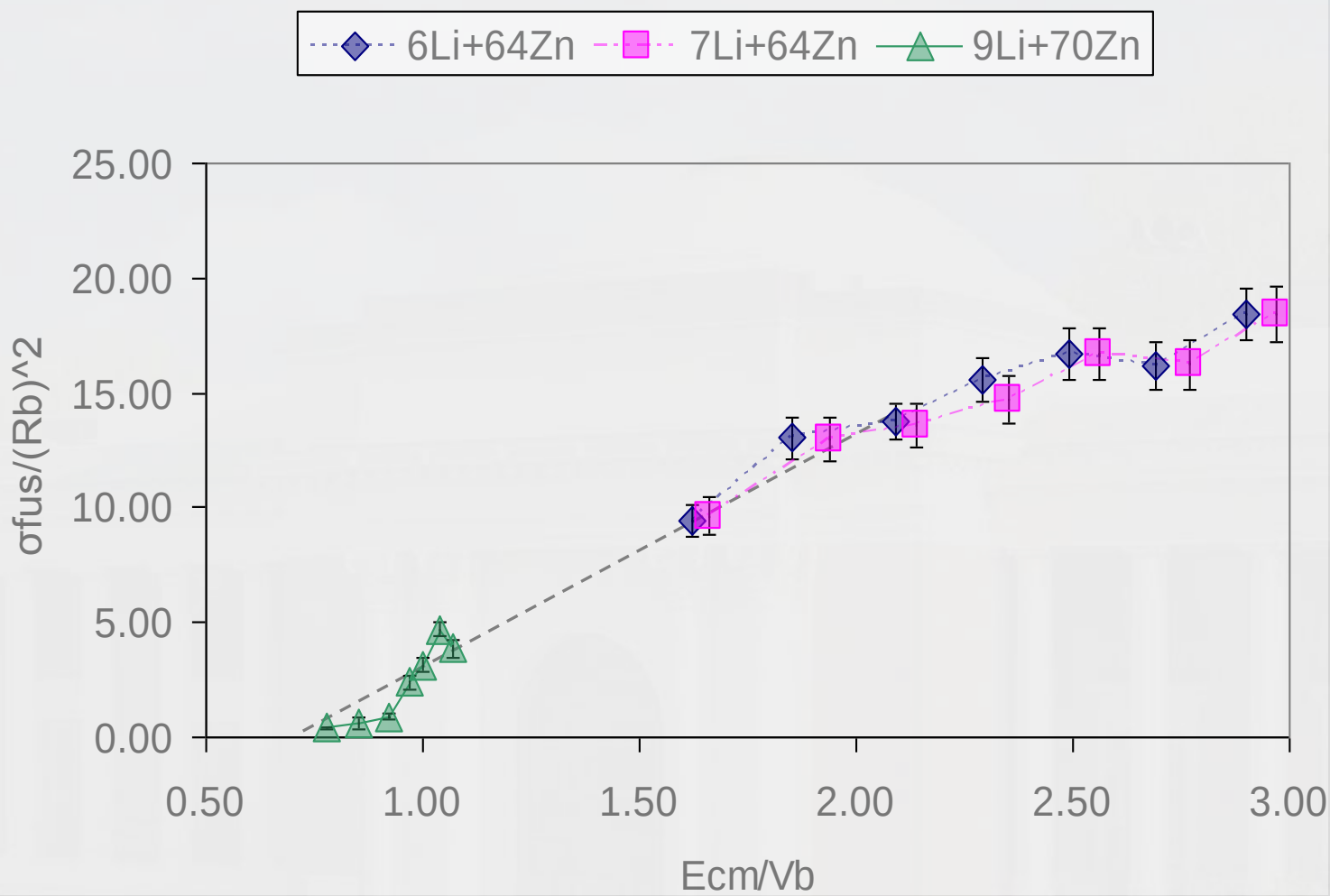

Sub-barrier fusion enhancement

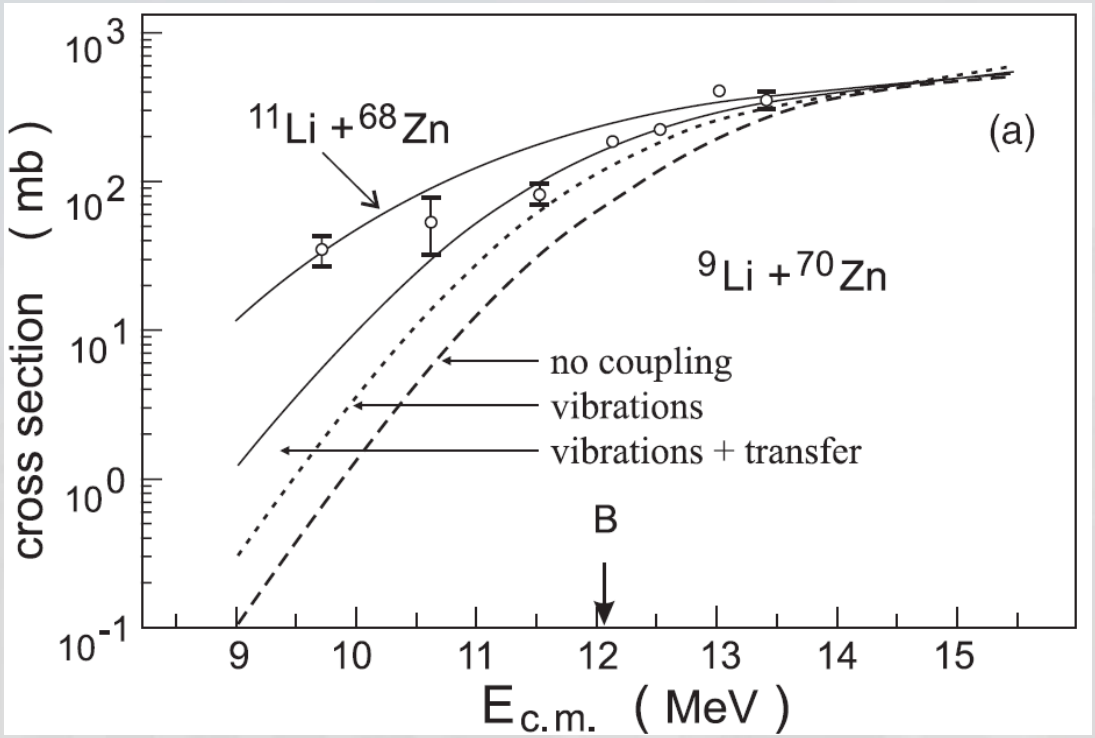

Source: *Zagrebaev 2007*

$$^{9}Li + ^{70}Zn \rightarrow ^{7}Li + ^{72}Zn$$

Q-value = +8.612MeV

Wong formula fit and R_B

$$\sigma_W = \frac{\hbar\omega_B R^2{}_B}{2E} \ln\left\{1+\exp\left[\frac{2\pi}{\hbar\omega_B}(E-V_B)\right]\right\}$$

- Values obtained by this fit (V_B fixed at 12.5MeV) are,
  Fusion radius (R_B) = 12.1±1.0fm
  Barrier curvature (ħω) = 5.7MeV
- Attributed to the existence of 'neutron skin'.
- Necessary to take into account sub-barrier fusion enhancement in ^{9}Li while explaining the same for ^{11}Li.

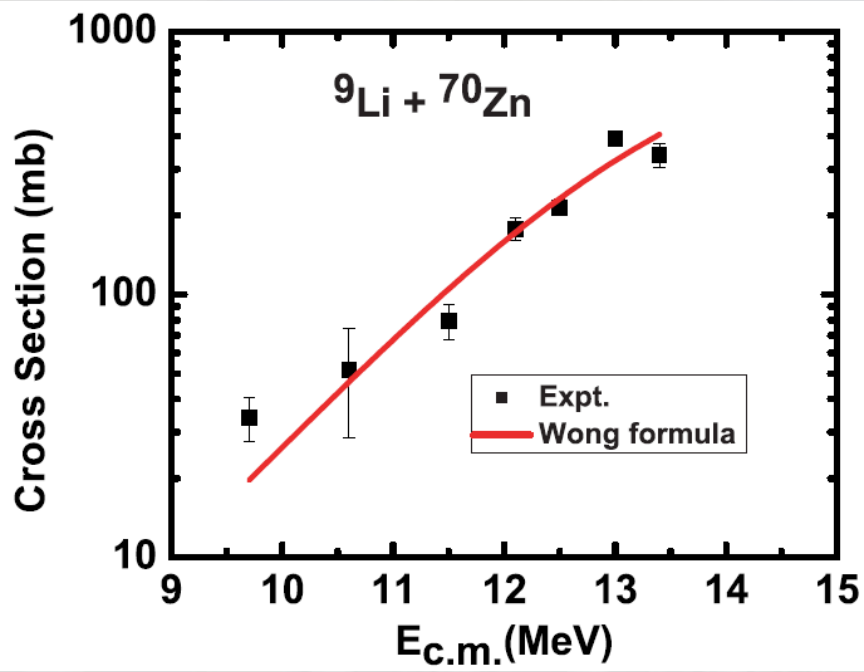

^{11}Li results

Nuclide	E_{lab} (MeV)	Target thickness (mg/cm^2)	Energy loss (MeV)	E_{cot} (MeV)	Beam dose (particles)	Average beam intensity (particles/s)
^{11}Li	17.5	1.25	0.5	17.0	1.19×10^8	7.79×10^2
	17.5	0.95	0.4	17.1	2.06×10^8	1.07×10^3
	16.5	0.99	0.4	16.1	7.77×10^7	4.56×10^2

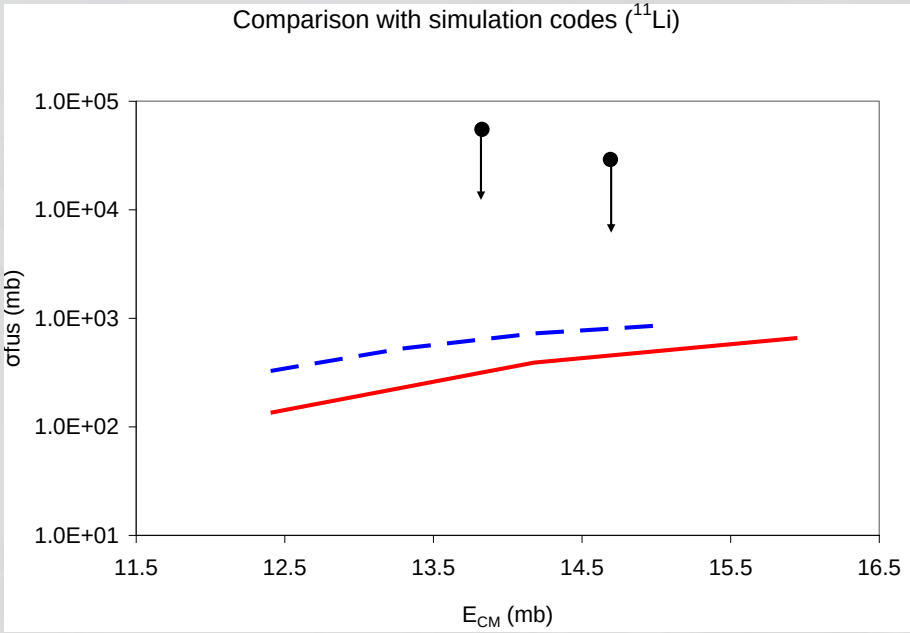

Projectile	E_{lab} (MeV)	Analysis method	σ_{fus}-β^* (mb)
^{11}Li	16.5	β	<55000
	17.5	β	<27000

*Upper limit cross section

Future work

Improvements?

- Experiments at beam energies lower than the ones used in present work to determine the limit of the sub-barrier fusion.
- For the $^{11}Li+^{70}Zn$ fusion reaction, need of similar experiments being done with much larger beam intensities in order to obtain reliable statistics.

Oregon State UNIVERSITY OSU

Acknowledgements

Funding bodies

- OSU Chemistry Department
- The David P. Shoemaker Memorial Fellowship, The Benedict Award
- The Director, Office of Energy Research
- Division of Nuclear Physics, Office of High Energy and Nuclear Physics, U.S. Department of Energy
- TRIUMF
- The Natural Sciences and Engineering Research Council of Canada

•Dr. Walter Loveland

•Argonne National Lab (ANL): Don Peterson, Partha Choudhary, Frank Moore, C. Jiang, Shrabani Sinha, Xodong Tang, S. Zhu, John Greene, Richard Pardo and the cyclotron operations staff.

•Tri-University Meson Facility (TRIUMF): Mike Trinczeck, Marik Dombsky, Peter Machule, Dave Ottewell, David Cross, Kate Gagnon, and William. J. Mills, Bob Laxdal, Marco Marchetto, Anne Trudel, Dave Hutcheon, the cyclotron operations and health physics staff.

•Dr. Phil Watson, Dr. Vince Remcho, Dr. Wei Kong and Dr. Kathryn Higley

•OSU Nuclear Chemistry Group.

•Mike Conrady, Lucas Hart (computer support), Ted Hinke (machining), Scott Menn, Jim Darrough (RHP), Leah Minc (γ detectors), The faculty and staff of the Radiation Center and Chemistry Department at Oregon State University.

Family and friends

Oregon State University OSU

Thank you!